

**NASA TECHNICAL
MEMORANDUM**

NASA TM X-71804

NASA TM X-71804

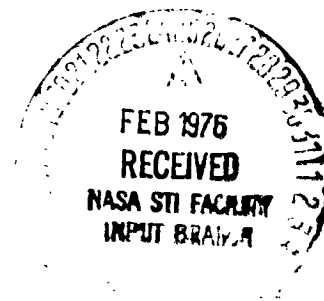
(NASA-TM-X-71804) ADVANCED TURBINE DISK
DESIGNS TO INCREASE RELIABILITY OF AIRCRAFT
ENGINES (NASA) 32 p HC \$4.00 CSCI 21P

N76-17143

Unclas
G3/07 14163

**ADVANCED TURBINE DISK DESIGNS TO INCREASE
RELIABILITY OF AIRCRAFT ENGINES**

by Albert Kaufman
Lewis Research Center
Cleveland, Ohio 44135



**TECHNICAL PAPER to be presented at
Gas Turbine Conference sponsored by the American
Society of Mechanical Engineers
New Orleans, Louisiana, March 21-25, 1976**

ADVANCED TURBINE DISK DESIGNS TO INCREASE
RELIABILITY OF AIRCRAFT ENGINES

by Albert Kaufman*

ABSTRACT

Results of analytical studies to improve the low cycle fatigue lives and reliability of turbine disks in high-performance gas turbine engines are presented. Advanced disk concepts were evaluated for the first-stage high pressure turbines of the CF6-50 and JT8D-17 engines. The advanced disk designs are compared to the existing disks on the bases of cycles to crack initiation and over speed capability for initially unflawed disks, crack propagation cycles to failure for initially flawed disks, and available kinetic energy of disk burst fragments.

INTRODUCTION

In this paper, some advanced disk concepts are analytically evaluated as to their potential for improving low cycle fatigue life and reliability of aircraft gas turbine disks. A disk burst is usually the most catastrophic failure possible in an aircraft engine. Statistics compiled by the Naval Air Propulsion Test Center on engine failures in U.S. commercial aviation^{1,2} show that of approximately 8000 engines in service,

*NASA Lewis Research Center, Cleveland, Ohio 44135.

¹DeLucia, R. A., and Mangano, G. J., "Rotor Burst Protection Program: Statistics on Aircraft Gas Turbine Engine Rotor Failures that Occurred in U.S. Commercial Aviation During 1972," Naval Air Propulsion Test Center Report NAPTC-PE-40, NASA CR-136900, Mar. 1974.

²Mangano, G. J., and DeLucia, R. A., "Rotor Burst Protection Program: Statistics on Aircraft Gas Turbine Engine Rotor Failures that Occurred in U.S. Commercial Aviation During 1973," ASME Paper no. 75-GT-12.

there were three turbine, two compressor, and three fan disk failures in 1972 and two turbine and four compressor disk failures in 1973; all of these failures, with the exception of one compressor disk failure, resulted in fragments piercing and escaping the engine casing. As the trend toward higher blade tip speeds and turbine inlet temperatures continues for military and commercial gas turbine engines, it is becoming more difficult to design reliable turbine disks satisfying both the life and performance requirements of the engines.

A possible solution to this problem which has been investigated^{3,4} is to protect the passengers and critical parts of the aircraft such as fuel lines from the effects of a disk burst by containing the damage within the engine. However, the containment devices required to afford adequate protection would impose a severe weight and, therefore, performance penalty on the engine.

The objective of this study was to increase disk reliability by utilizing advanced structural and fabrication concepts to improve low cycle fatigue life, increase crack propagation resistance, and reduce the

³Mangano, G. J., "Rotor Burst Protection Program. Phases VI and VII: Exploratory Experimentation to Provide Data for the Design of Rotor Burst Fragment Containment Rings," Naval Air Propulsion Test Center Report NAPTC-AED-1968, AD-744950, Mar. 1972.

⁴Yeghiayan, R. P., Leech, J. W., and Witmer, E. A., "Experimental and Data Analysis Techniques for Deducing Collision-Induced Forces from Photographic Histories of Engine Rotor Fragment Impact/Interaction with a Containment Ring," Mass. Inst. of Tech. Report ASRL-TR-154-5, NASA CR-134548, Oct. 1973.

fragment energies that would be generated in the event of a disk failure. Under contract to NASA, the General Electric Company and Pratt & Whitney Aircraft evaluated a number of disk concepts and designed new disks as potential replacements for the existing first stage, high pressure turbine disks of the CF6-50 and JT8D-17 turbofan engines, respectively. The approach used in the CF6-50 disk program was to increase fatigue life and reduce fragment energy by utilizing a redundant construction at the cost of extra disk weight. In the JT8D-17 disk program the emphasis was on improving the cyclic life without providing redundancy or increasing the disk weight. The cycles to crack initiation and the overspeed capability for initially unflawed disks, the cycles required to propagate initial flaws to failure, and the available kinetic energy of disk burst fragments were compared for the advanced disk designs and the existing disks using both conventional and advanced materials.

ADVANCED DISK CONCEPTS

CF6-50 Designs

The existing first stage turbine disk (henceforth called the "standard disk") and the candidate disk designs considered as potential replacements are illustrated in Fig. 1. The standard disk (Fig. 1(a)) is machined from an integral forging of Inconel 718 alloy. Cooling air is brought from the compressor through the disk bore, pumped up radially through a liner between the stage 1 and 2 disks, and then channeled around the bolt holes to the disk rim and into the blades through holes in the blade dovetails. Local bosses provide reinforcement around the bolt holes to increase the low cycle fatigue lives at the hole rims. The bore-entry disk (Fig. 1(b)) is a split disk with the two disk halves connected by inte-

gral radial webs for channeling coolant up the center of the disk from the bore to the blades; this improves the cooling effectiveness and minimizes axial thermal gradients. Another attractive feature of this concept is the increased resistance to propagation of cracks or flaws in the axial direction. It is envisaged that the bore-entry disk would be fabricated from an integral forging using electrochemical machining to produce the cavities between the disk halves and the radial webs.

The composite disk (Fig. 1(c)) utilizes high-strength filament or wire hoops to provide most of the load-carrying ability of the disk except at the blade attachments. The hoops would have to be under an initial pretension in order to assure that the loading was properly distributed among the filaments; this could be accomplished by filament winding techniques, by interference fitting the hoops on the disk halves or by selecting a combination of fibrous and matrix materials with differential thermal expansions which would apply the desired hoop pretension under engine operating conditions. The main attractions of this concept are a high strength-to-weight ratio and a high degree of load-carrying redundancy.

The laminated and link disks (Figs. 1(d) and (e)) are oriented toward insuring load-carrying redundancy, isolation of propagating cracks, and generation of small burst fragments rather than improving design life. The two concepts are basically similar except that ring-type laminates are bolted together in one case and layers of link segments are pinned together in the other case. Cost reductions over forged and machined disks could be achieved by fabricating these disks using sheet metal stamping and die-punching techniques.

The multi-bore disk (Fig. 1(f)) separates the highly stressed bore region into a number of circumferential ribs in order to prevent a crack or flaw at the bore from propagating in the axial direction. In order to accommodate the spaces between the ribs, the thickness of the disk at the bore has to be increased substantially over that of the standard disk.

The multi-disk concept (Fig. 1(g)) is composed of three or more disks bolted together and designed so that if one disk fails, the others can temporarily carry the blade loads. Fig. 1(g) illustrates a four-member multi-disk design. Each member can be shaped for a more efficient utilization of material than is possible with a disk fabricated from sheet metal laminates. As in the bore entry disk, cooling air can be brought through the bore and pumped up radially between disk members to the blade attachments.

The spline disk (Fig. 1(h)) consists of two disk halves which are splined together and each designed to temporarily carry the tangential load of the other in case of failure. In order to counter the tendency of each disk half to straighten out due to lack of symmetry about the axis, the splines would be radially interlocked by means of diamond-shaped rods. The mechanical coupling of the disk halves prevents a crack from propagating from one disk to the other and tends to contain failed disk segments within the splines of the undamaged disk.

All the disk concepts involving forgings would be fabricated from Rene 95 and all those involving sheet metal members would be made from Rene 41.

JT8D-17 Designs

Fig. 2(a) shows the existing or "standard" first stage turbine disk.

This disk is machined from a Waspaloy forging. Cooling air is bled from the combustion liner and discharged at high velocity through nozzles toward the disk rim on the front side of the disk. Angled holes at the disk rim channel the coolant to the blades; these holes result in elliptical exit openings with high stress concentrations which are the limiting low-cycle fatigue failure locations in the standard disk.

A split-bonded disk concept (hereafter called the "design disk" for the JT8D-17 engine) was selected as a possible replacement for the standard disk. In some respects, the split-bonded disk shown in Fig. 2(b) is similar to the bore entry disk (Fig. 1(b)) considered for the CF6-50 engine. As in the latter case, cooling air would be introduced at the bore, pumped up radially between disk halves through channels formed by radial webs, and supplied to each blade through radially oriented exit holes at the disk rim. Instead of having an integral disk as in the bore-entry design, the two halves of the bonded disk would be fabricated from separate Astroloy forgings which would then be diffusion-brazed together at the center surfaces of the radial webs using a braze alloy of similar composition to Astroloy with the addition of a melting point depressant. Dovetail broaching and final machining operations would be performed on the bonded disk assembly.

DISK ANALYSIS

Design Conditions

Design properties of the disk materials for the candidate disk concepts are shown in Table I. The simplified flight cycles used for the analyses of the CF6-50 and JT8D-17 disks are shown in Figs. 3 and 4, respectively, in terms of inlet Mach number, altitude, turbine inlet tem-

perature and engine speed versus flight time.

Crack Initiation

Transient temperatures were computed throughout the design and standard disks from three-dimensional heat transfer computer programs. Radial, tangential, and axial stresses were calculated from three-dimensional finite element computer programs. Detailed stress analyses were also performed for the disk dovetail attachments to the blades. The number of cycles required to initiate cracks of 0.076 to 0.082 cm (0.030 to 0.032 in.) length at critical locations was determined from the results of the thermal and stress analyses of unflawed disks and from mechanical stress or strain cycling data obtained in tests of laboratory specimens.

Crack Propagation

The cycles required for a crack to grow from an initially assumed flaw to a critical size or to failure were computed by means of fracture mechanics theory. The computation was performed by a numerical integration over the flight cycle using the empirically determined relation between crack growth rate and stress intensity at the crack tip for a given stress range. Crack propagation lives for the CF6-50 disks were based on the growth of a semi-elliptical surface flaw 0.635 cm (0.250 in.) long by 0.212 cm (0.0833 in.) deep; the rationale for considering such a relatively large flaw size was that experience has shown that such flaws in turbine disks have occasionally escaped detection through human error. Semi-elliptical surface flaws were also assumed for crack-initiation limited critical regions of the JT8D-17 disks, but with crack lengths of 0.0826 cm (0.0325 in.) corresponding to the crack initiation design criteria used for the JT8D-17 disk designs. In addition, effects of circular

subsurface flaws in the bore region and of discontinuities along the web bond surface of the disk due to misalignment of the two disk halves were analyzed; a sonically detectable diameter of 0.119 cm (0.047 in.) was assumed for the subsurface flaws. All flaws were oriented so that the plane of the crack front was normal to the maximum principal stress direction. Fracture mechanics analyses were performed for the most critical locations on each standard and design disk.

Overspeed Capability

Burst speeds of the disks were determined from empirical correlations of spin pit test results with the disk tangential stresses and minimum ultimate tensile strengths based on average disk temperatures. Overspeed capability was established by comparing the disk burst speeds to the maximum takeoff speed of the engine.

All computations were performed for the standard disk, the design disk, and the standard disk using the same advanced material as the design disk (henceforth called the "advanced standard disk").

DISCUSSION OF RESULTS

Analyses of CF6-50 Disk Concepts

The results of the preliminary analyses to screen the candidate turbine disk concepts for the CF6-50 engine are summarized in Table II.

The bore entry disk has greater burst and low cycle fatigue capability than the standard disk because of the improved transient thermal response and sizing each disk half to carry the load of the other in case of failure. However, the redundant design results in a significantly heavier disk. If each disk half were sized to have the same stress levels as the standard disk, there would be an 86 percent increase in disk

weight, which would increase the SFC about 0.29 percent for an average flight. Resistance to flaw propagation is substantially improved since the disk halves are only connected by the webs. The probability of a flaw propagating through a web in the bore region is only 1 in 5 on the basis of the ratio of the web width to the bore circumference.

The composite disk has lower stress levels and a longer cyclic life for the same weight than the standard disk because of the extra load-carrying ability of the wire or filament hoops. In order to operate in the CF6 environment, the hoop material would have to be able to carry a stress of about 138 000 N/cm² (200 000 psi) at a temperature of 811 K (1000° F). A survey of fiber materials has found only a few with the required temperature-stress capability and extensive fabrication development would be required to demonstrate that these could be utilized in a practical design.

The laminated disk exhibits extremely high stresses in the bolts and around bolt holes in the laminates due to nonuniform load distribution in the axial direction. High thermal stress gradients through the disk thickness are also likely to be a problem due to differences in the thermal responses of the inner and outer laminates. Another negative feature of the laminated design is the excessive weight due to the difficulty of utilizing the sheet material efficiently.

The link disk was found to have very high tensile and bending stresses and the links could not support the centrifugal loading at the CF6 operating conditions. This design appears to be unsuitable for turbines in advanced engines although it may be practicable for fan or compressor disks.

The analysis of the multi-bore disk revealed high transient thermal stresses at the rib outer diameter rather than the low stresses that had been expected. The desired benefit of this design in retarding the propagation of rim flaws was, therefore, not fully realized.

The multi-disk design was analyzed for redundancy under various failure conditions. It was found that the bolts would not be able to support a failed outer disk. Analysis also indicated that a flawed center disk would probably reach critical length before a significant proportion of the load could be redistributed through the bolts to the undamaged disk members.

The spline disk presents special problems in analysis because the load distribution among the splines is dependent on the fabrication tolerances and it is not apparent how the loading would be redistributed when a part failed.

As a result of the preliminary analysis, only the bore-entry, composite and spline concepts were considered suitable for CF6 turbine disk applications. From a strength and life standpoint, the composite disk is the most promising concept; however, because of the fabrication problems involved, this design was not further considered. The bore-entry disk (henceforth called the "design disk" for the CF6-50 engine) was selected for further study over the spline disk because its integral construction gives more assurance that loading due to a failed part would be more evenly redistributed and because cooling of the spline disk presents more problems.

The rim and bore temperature responses of the standard and design disks during the flight cycle are shown in Fig. 5; average effective stresses for various flight times are also indicated. In both disks, the

maximum rim temperatures occur at the end of takeoff and maximum bore temperatures occur during climb. Bore temperatures in the design disk are only slightly cooler than in the standard disk since the bore is cooled in both disks. Rim temperatures are higher in the design disk because the coolant picks up heat as it flows radially up the center of the disk whereas the coolant in the standard disk does not come into contact with the sides of the disk until it reaches the bolt holes.

Fig. 6 shows the critical locations where manufacturing flaws were assumed for the standard and design disks. The dovetail post rabbet which has the limiting low cycle fatigue life was not considered since failure at this location would not generate high energy fragments. These critical locations were at the dovetail slot bottom, bolt hole, and bore for both disks and, in addition, at the web-disk junction near the bore in the design disk. The calculated number of cycles to crack initiation for initially unflawed disks and of cycles to failure for initially flawed disks at the critical locations are summarized in Table III. These results indicate a significant improvement in the low cycle fatigue lives of the advanced standard and design disks because of the improved crack initiation characteristics of the advanced material. The initial FAA approved life for the standard disk is 7800 cycles, which will be increased subject to the results of three fleet leader engines.

The most critical locations for flaws were at the dovetail slot bottom in the standard disk and at the bore in the advanced standard and design disks. Although the flawed design disk (with a bore flaw) shows an improvement of more than 300 percent in cyclic life over the standard disk (with a flaw at the dovetail slot bottom) in Table III, part of this

increased life is the result of improved material properties. If the effect of different materials is removed by comparing the bore-flawed design disk with the bore-flawed advanced standard disk, the improvement in life due to the structural concept alone is 136 percent because of the redundant construction of the design disk. Table III also shows that there is an improvement in the overspeed capability of the design disk of 18 percent over the standard disk and 11 percent over the advanced standard disk.

The life of the standard disk could also be increased by adding to it the extra 86 percent of weight shown in Table III for the design disk. However, a heavier standard disk would lack the redundancy of the design disk and would generate even higher fragment energies in the event of premature disk burst due to the presence of a flaw.

The available kinetic energies for the most likely fragment patterns from failures originating at the flaw locations are presented in Table IV. An assumption of these analyses was that the redundant construction of the design disk would prevent catastrophic failure due to the propagation of a radial crack from bore to rim; therefore, no kinetic energy is shown as resulting from bore failures in the design disk. The maximum energy of fragmentation in the design disk is only 7 percent of that in the standard and advanced standard disks; this reduction in fragment energy would considerably reduce the containment problem.

Analyses of JT8D-17 Disk Concepts

Fig. 7 shows the rim and bore temperatures with respect to the flight cycle for the standard and design disks and indicates effective stresses at various times during the cycle. The maximum temperatures at

both bore and rim occur at the end of takeoff. Since the coolant is delivered by a tangential on-board injection system in this engine and only the rim of the standard disk is cooled, the relative thermal responses for the standard and design disks are different from those for the CF6-50 engine. Fig. 7 shows that bringing the coolant through the bore of the JT8D-17 design disk results in a significant temperature reduction in the bore region as compared to the standard disk. Disk stresses are lower than those shown in Fig. 5 for the CF6-50 disk, because the JT8D-17 disk has a lower rim velocity.

The critical locations for manufacturing flaws in the JT8D-17 standard and design disks are indicated in Fig. 8. Subsurface flaws were assumed in the standard disk at the bore region and at the maximum radial stress location in the web and in the design disk at the bore region. Surface flaws were assumed at the rim cooling air exit hole in the standard disk and at the bore cooling air entrance in the design disk. In addition, a flaw was considered in the design disk at the maximum axial stress location on the bond surface; this flaw would result from formation of a sharp corner due to a misalignment of the web of the two disk halves during bonding.

Results of the crack initiation, crack propagation, and burst speed calculations for the standard, advanced standard, and design disks are presented in Table V. These results show an improvement in the low cycle fatigue life of the design disk of 88 percent over the standard disk and 67 percent over the advanced standard disk. The low cycle fatigue life of the standard disk shown in Table V is the FAA certified life of the disk.

The crack propagation results in Table V show a reduction in life for the advanced standard disk as compared to the standard disk. This reduction is due to the fact that the crack propagation rates for forged Astroloy are greater than those for Waspaloy; there are preliminary indications that the crack propagation properties of powdered Astroloy may be superior to those of the forged material. The most critical locations for crack propagation were at the limiting low-cycle fatigue crack-initiation sites, i.e., at the cooling air exit holes for the standard and advanced standard disks and at the cooling air entrance in the design disk. The improvement in the limiting crack propagation life for the design disk over the standard disk was 124 percent. The fragment energies shown in Table VI for the JT8D-17 disks show that a reduction of 50 percent in the maximum fragment energies is achievable with the design disk.

CONCLUDING REMARKS

A number of disk structural designs have been studied as potential replacements for the existing first-stage turbine disks in the CF6-50 and JT8D-17 engines. A bore-entry design was selected for the CF6-50 disk as a result of preliminary analyses of seven design concepts including composite, laminated, link, multi-bore, multi-disk, and spline designs. The bore-entry design was designed to improve disk life and prevent high fragment energy failure by utilizing a redundant construction at the expense of an increase in disk weight. The split-bonded disk concept selected for evaluation for the JT8D-17 engine is similar in some respects to the bore-entry concept, but was designed to improve disk life without redundancy or increase in disk weight. Differences in design philosophy, fab-

rication procedure, disk cooling, and engine operating characteristics influence the resultant benefits of each design. Cyclic thermal and stress analyses of these disks revealed that substantial improvements in low cycle fatigue lives of both unflawed and initially flawed disks could be achieved for both engines by replacing the existing first stage turbine disks with the candidate disk designs.

ACKNOWLEDGMENT

These studies were performed by the General Electric Company and Pratt & Whitney Aircraft under contract to NASA. The author is grateful to R. H. Andersen and A. S. Alver who served as Project Managers for the CF6 50 and JT8D-17 programs, respectively.

TABLE I. - DESIGN PROPERTIES OF TURBINE DISK MATERIALS

Property	CF6-50 engine		JT8D-17 engine	
	In 718	Rene 95	Waspaloy	Astroloy
Ultimate tensile strength, N/cm ² 294 K 811 K	126 000	150 000	124 000	134 000
	110 000	145 000	110 000	117 000
Yield strength (0.2% offset), N/cm ² 294 K 811 K	101 000	116 000	86 000	97 000
	92 000	110 000	76 000	87 000
Elongation at failure, percent 294 K 811 K	20	8.5	24	19
	20	8.5	21	14.5
1000 hour rupture strength, N/cm ² 867 K	68 000	103 000	79 000	84 000
Stress range for crack initiation in 1000 cycles, (min stress = 0 N/cm ²), N/cm ² 811	81 000	93 000	85 000	85 000
Critical stress intensity factor, N/cm ^{3/2} 894 K	93 000	88 000	>68 000	>68 000

^aEstimated.

TABLE II . RESULTS OF PRELIMINARY ANALYSES OF CF6-50 DISK CONCEPTS

Disk concepts	Advantages	Disadvantages
Bore entry	Redundancy, improve thermal response, longer life	Increased weight to provide redundant design
Composite	Reduced stress levels, longer cyclic life	Limited material possibilities, fabrication development required
Laminated	Redundancy, low fragment energy, low cost	Excessive weight, high stresses at bolts and bolt holes, thermal mismatches between laminates
Link	Redundancy, low fragment energy, low cost	Excessive link stresses, difficult to seal disk to prevent coolant leakage
Multi-bore	Ribs prevent axial flaw propagation at bore	High transient thermal stresses at rib outer diameter
Multi-disk	Improved thermal response, some redundancy	Excessive weight, concern over rotor spool integrity if outer disk failed
Spline	Redundancy, longer life	Increased weight

TABLE III. - RESULTS OF LIFE AND OVERSPEED ANALYSES F. R. CF6-50 TURBINE DISKS

Failure type	Standard disk (Inco 718)	Advanced standard disk (Rene 95)	Design disk (Rene 95)
Cycles to crack initiation in initially unflawed disk			
Dovetail post rabbet	30 000	Not calculated	>100 000
Bore	63 000	>100 000	>100 000
Dovetail slot bottom	>100 000	>100 000	>100 000
Bolt hole	>100 000	>100 000	>100 000
Cycles to failure in ini- tially flawed disk,			
Bore	611	662	1 564
Dovetail slot bottom	380	1 155	1 928
Bolt hole	1 809	7 161	34 026
Web-disk junction	---	---	1 673
Burst speed as percent of maximum takeoff speed	126	134	149
Weight change as percent of standard disk weight	---	0	b+86

^a Initial FAA approved life is 7800 cycles subject to increase as result of fleet leader testing.

^b Increased weight results from redundancy.

TABLE IV. - RESULTS OF FRAGMENT ENERGY ANALYSES FOR CF6-50 TURBINE DISKS

Fragment pattern	Flow location	Available kinetic energy, joules		
		Standard disk	Advanced standard disk	Design disk
90° disk segment	Bore	852 400	881 600	--- ---
120° disk segment	bore	1 172 500	1 175 500	--- ---
180° disk segment	Bore	1 758 700	1 763 200	--- ---
4 blades, 3 dovetail posts, disk segment between rim and bottom of bolt hole reinforcement	Dovetail slot bottom	110 300	110 500	116 000
4 blades, 3 dovetail posts, disk segment between rim and center of bolt holes	Bolt hole	107 200	107 300	111 200

TABLE V. - RESULTS OF LIFE AND OVERSPEED ANALYSES FOR JT8D-17 TURBINE DISKS

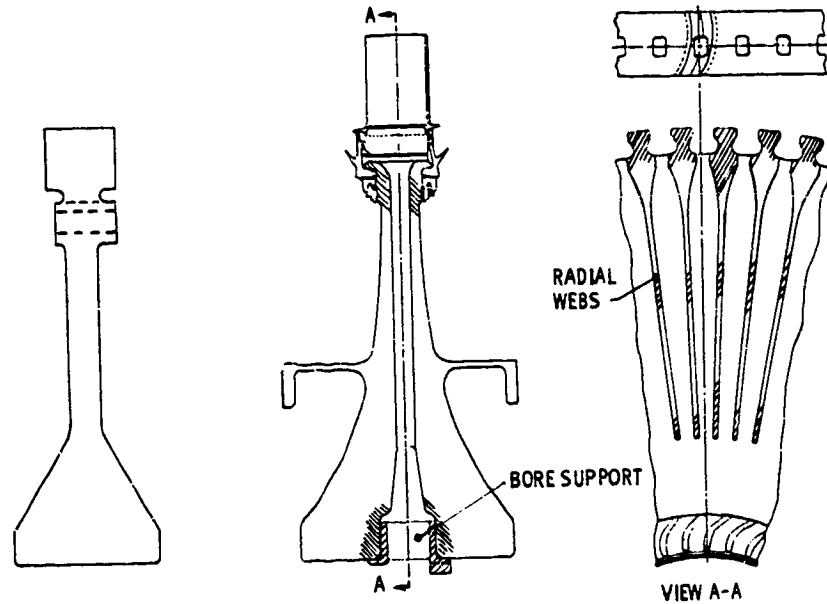
Failure type	Standard disk (Waspaloy)	Advanced standard disk (Astroloy)	Design disk (Astroloy)
Cycles to crack initiation in initially unflawed disk			
Bore	>100 000	>100 000	>100 000
Cooling air exit hole	16 000	18 000	35 000
Cooling air entrance	---	---	30 000
Cycles to failure in ini- tially flawed disk			
Bore	65 000	39 000	37 000
Web (max. radial stress loc.)	97 000	59 000	>100 000
Cooling air exit hole	2 900	1 150	---
Cooling air entrance	---	---	6 500
Burst speed as percent of maximum takeoff speed	136	136	133
Weight change as percent of standard disk weight	---	-4	0

^aFAA certified life.

TABLE VI. - RESULTS OF FRAGMENT ENERGY ANALYSES
FOR JT8D-17 TURBINE DISKS

Fragment pattern	Flow location	Available kinetic energy, joule		
		Standard disk	Advanced standard disk	Design disk
120° disk segment	Cooling air exit hole, web, bore	678 600	653 600	---
180° disk segment	Cooling air exit hole, web, bore	1 017 700	980 400	---
20 blades and dovetail posts, 90° segment of rear disk half	Web bond surface, cooling air entrance	---	---	441 400
27 blades and dovetail posts, 120° segment of rear disk half	Bore	---	---	513 000

E-8421



(a) STANDARD DISK.

(b) BORE-ENTRY DISK.

Figure 1. - CF6-50 first stage turbine disk designs.

PRECEDING PAGE BLANK NOT FILMED

**ORIGINAL PAGE IS
OF POOR QUALITY**

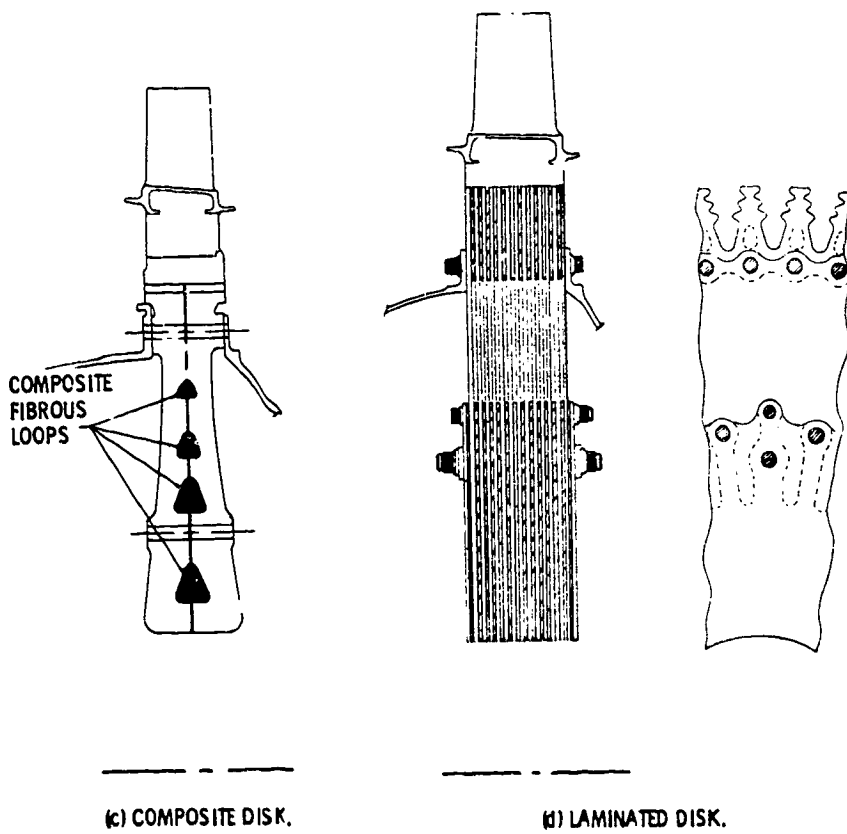
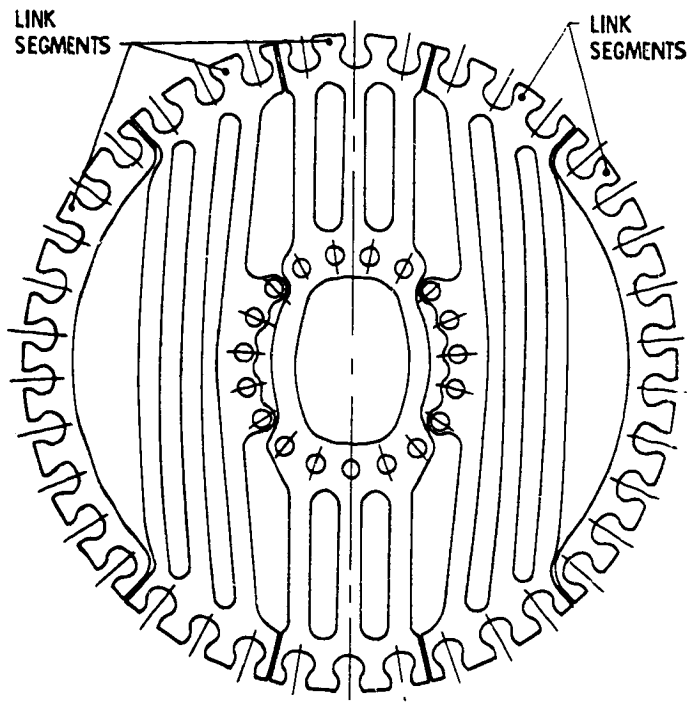


Figure 1. - CF6-50 first stage turbine disk designs.

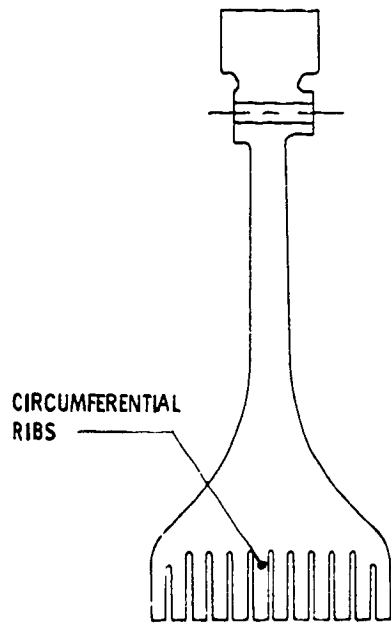
ORIGINAL PAGE IS
OF POOR QUALITY

I - 8491



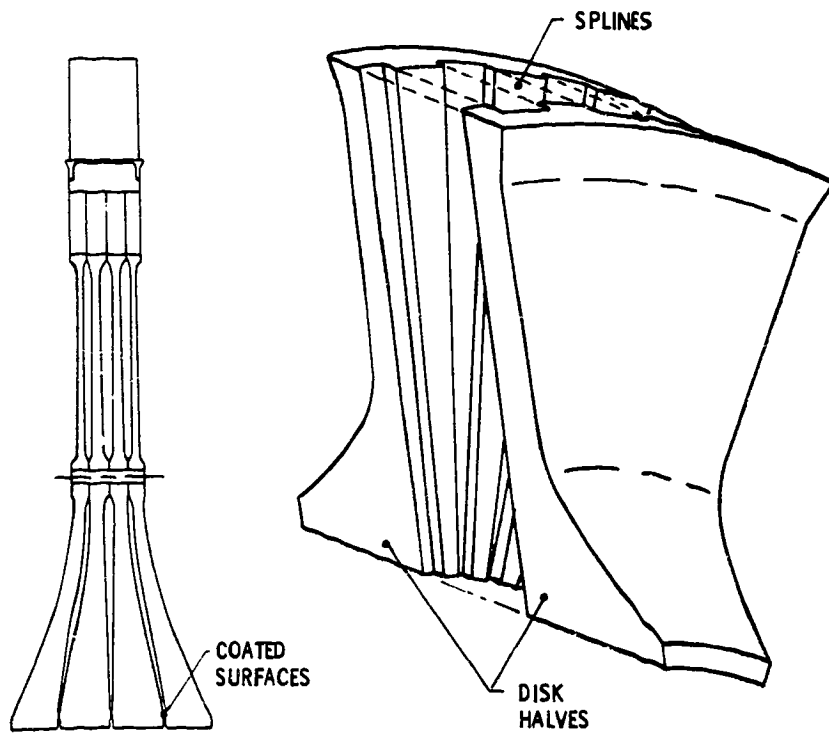
TYPICALLY A DISK WOULD CONTAIN 20 TO 40 LAYERS EACH Clocked AXIALLY RELATIVE TO THE NEXT.

(e) LINK DISK.



(f) MULTI-BORE DISK.

Figure 1. - CF6-50 first stage turbine disk designs.

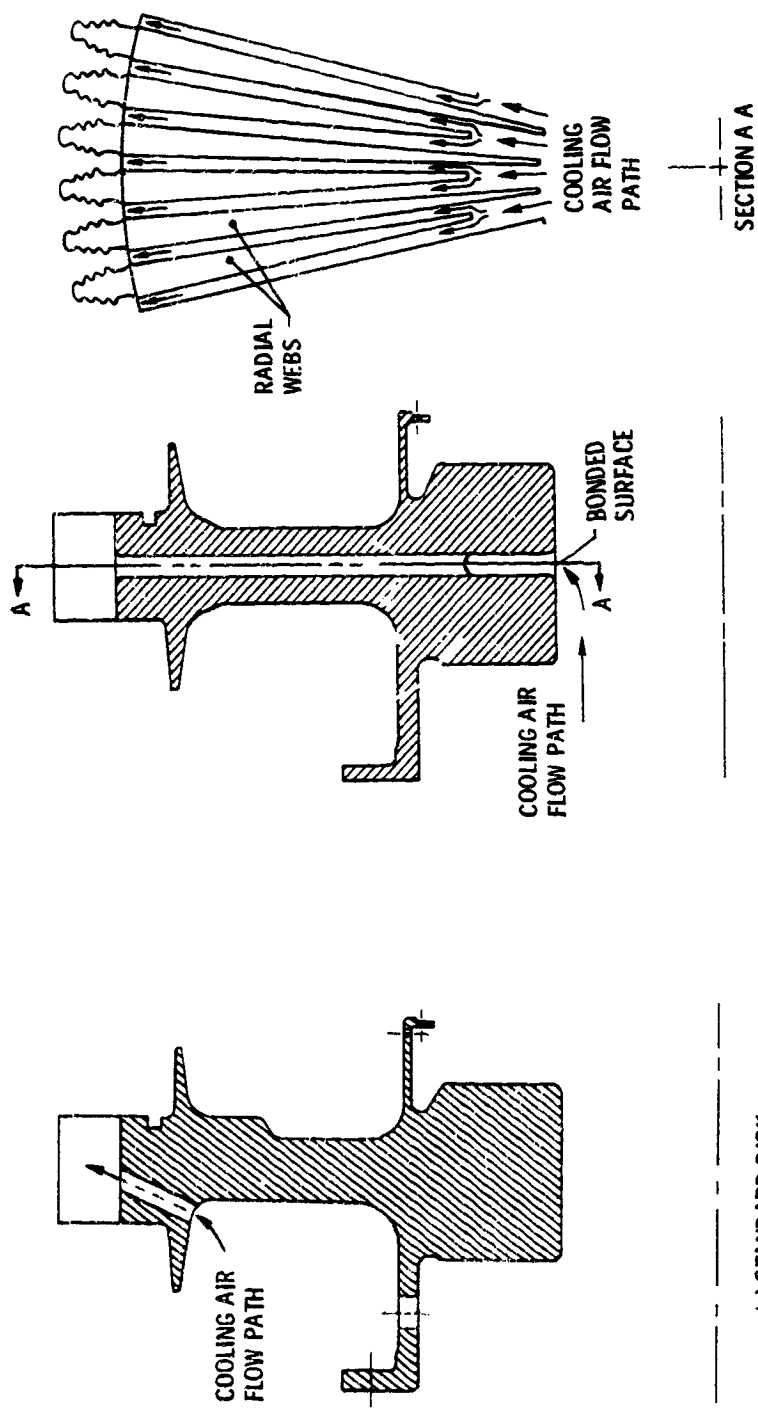


(g) MULTI-DISK.

(h) SPLINE DISK.

Figure 1. - CF-50 first stage turbine disk designs.

ORIGINAL PAGE IS
OF POOR QUALITY



(a) STANDARD DISK.

(b) SPLIT-BONDED DISK.

Figure 2. - JT8D-17 first stage turbine disk designs.

I-8191

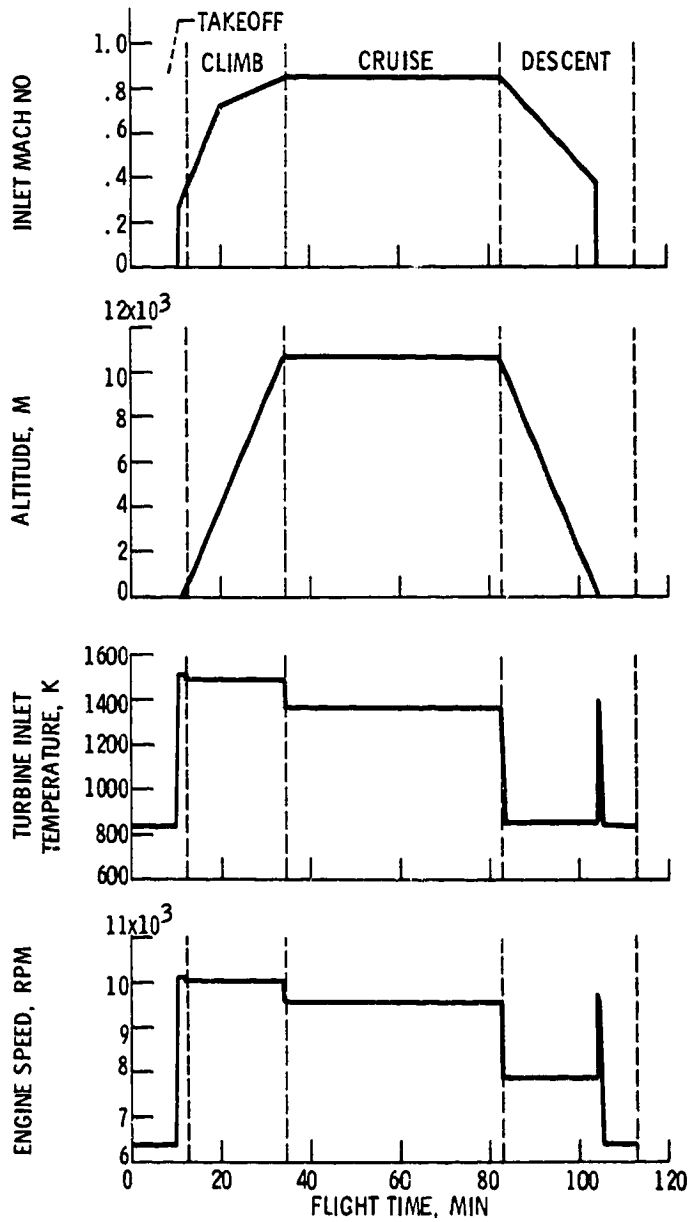


Figure 3. - CF6-50 simplified engine cycle.

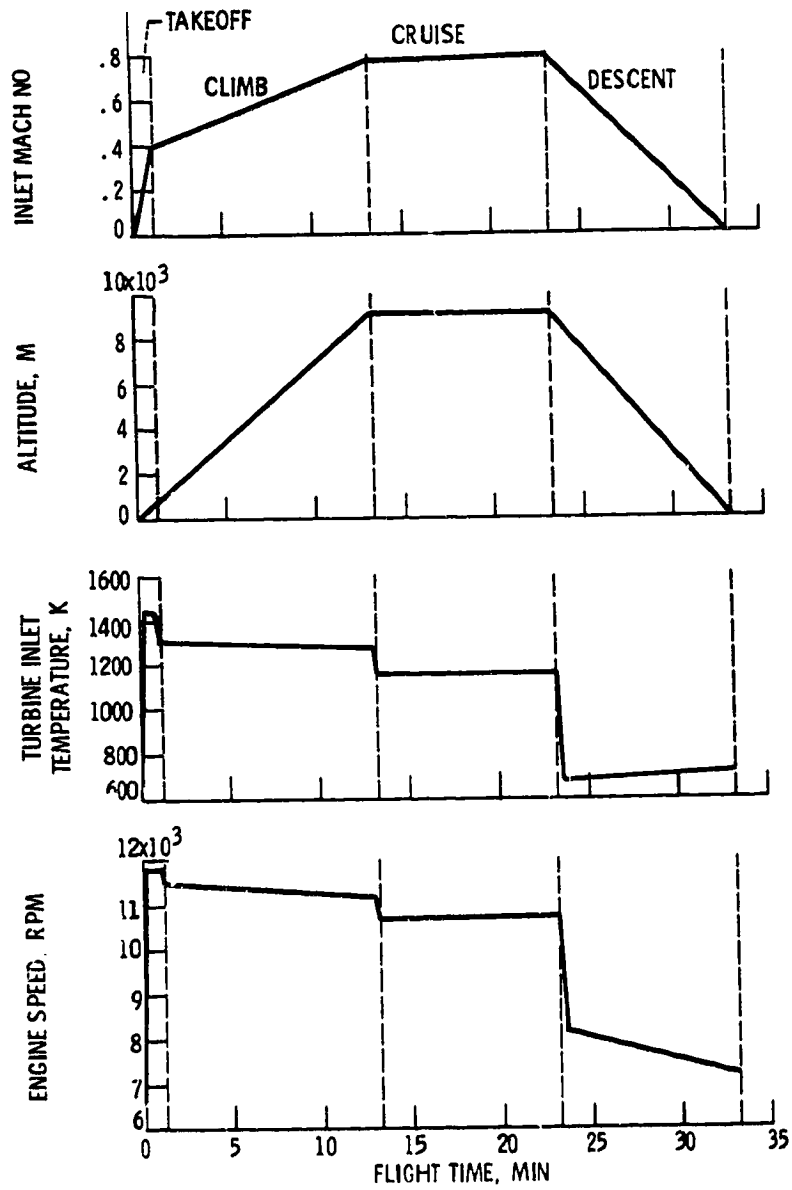


Figure 4. - JT8D-17 simplified engine cycle.

F-4491

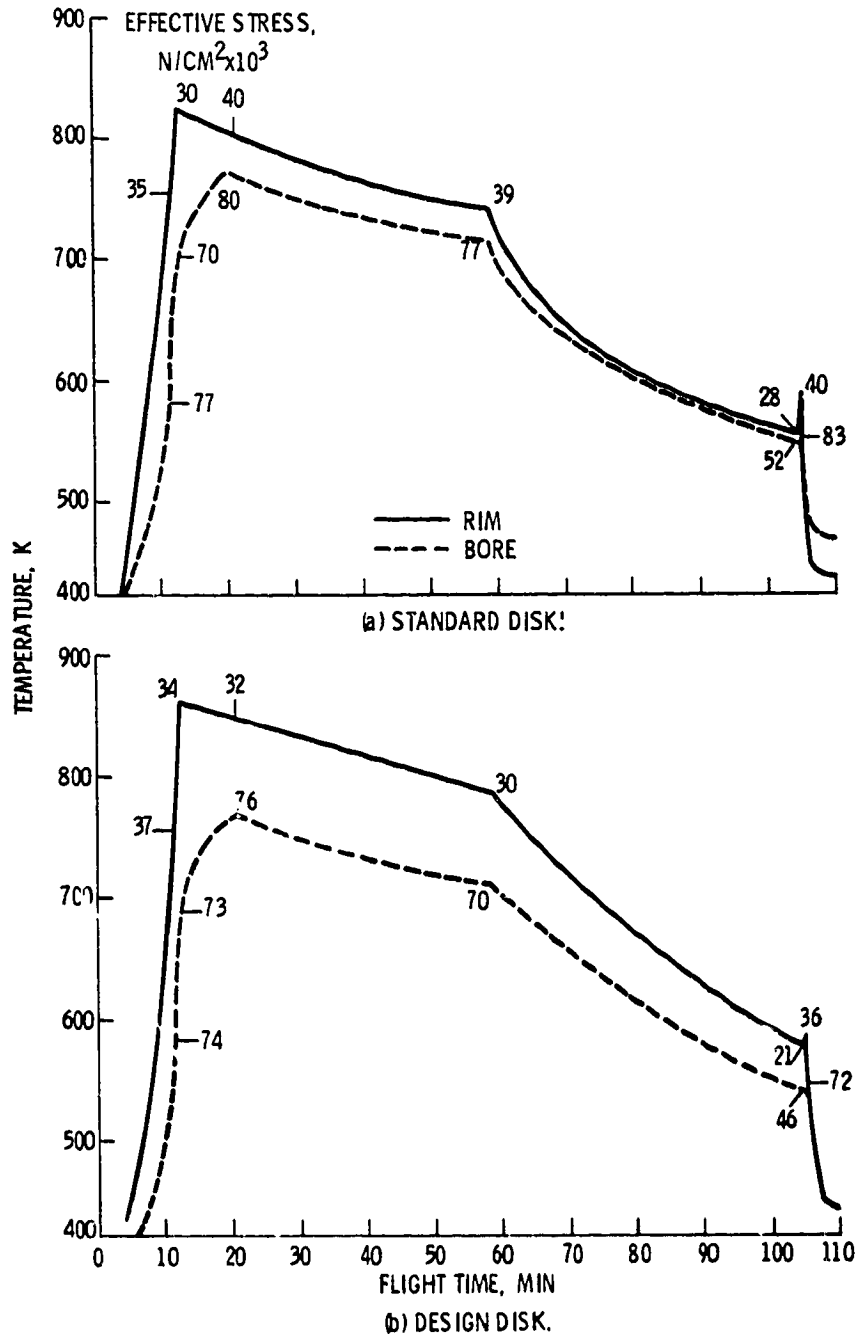


Figure 5. - CF6-50 turbine disk temperature response.

F-8491

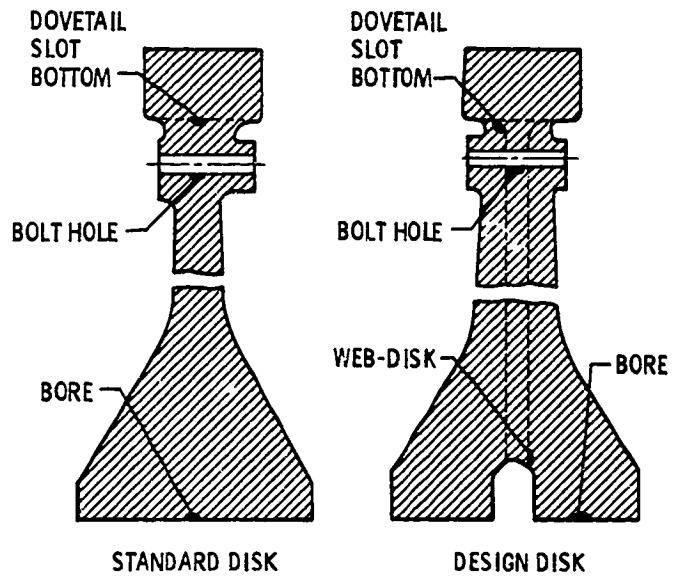


Figure 6. - CF6-50 turbine disk assumed initial flaw locations.

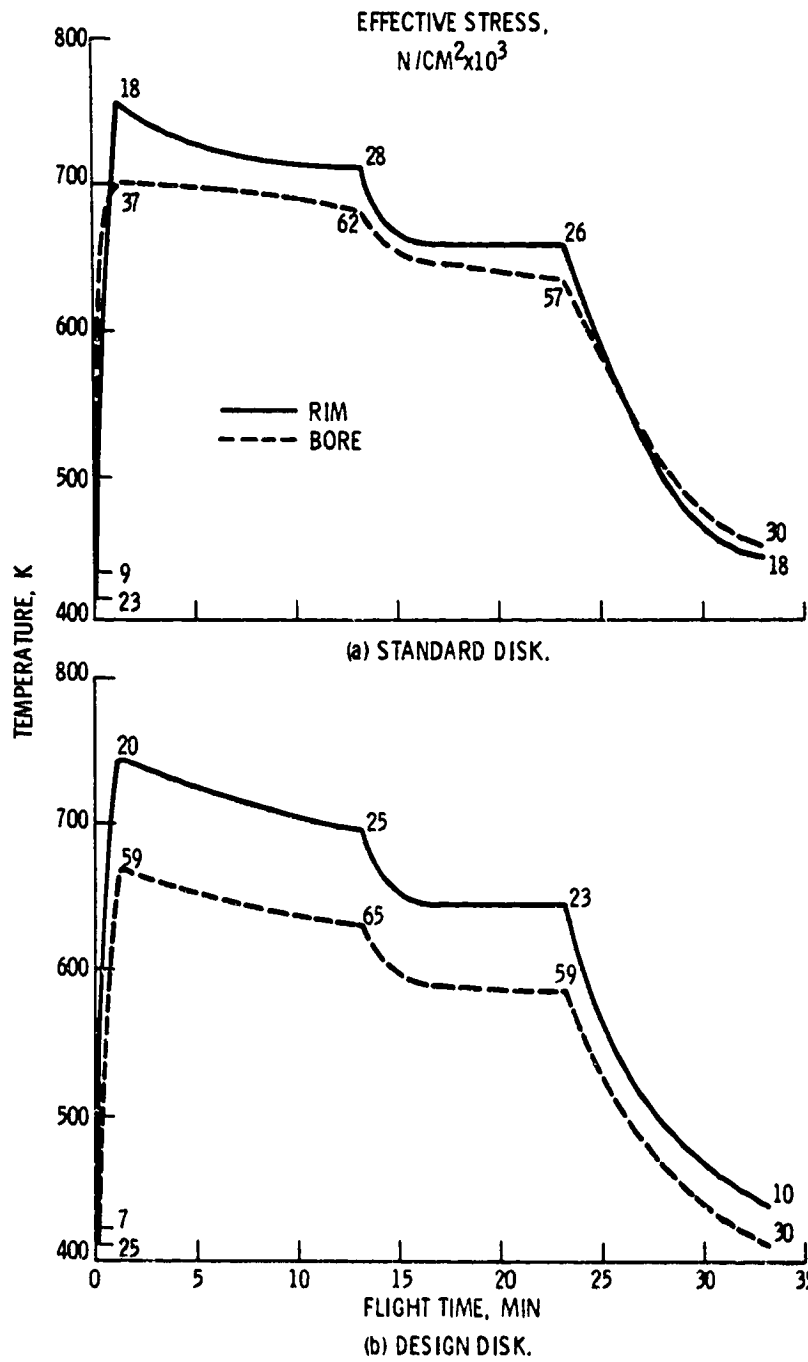


Figure 7. - JT8D-17 turbine disk temperature response.

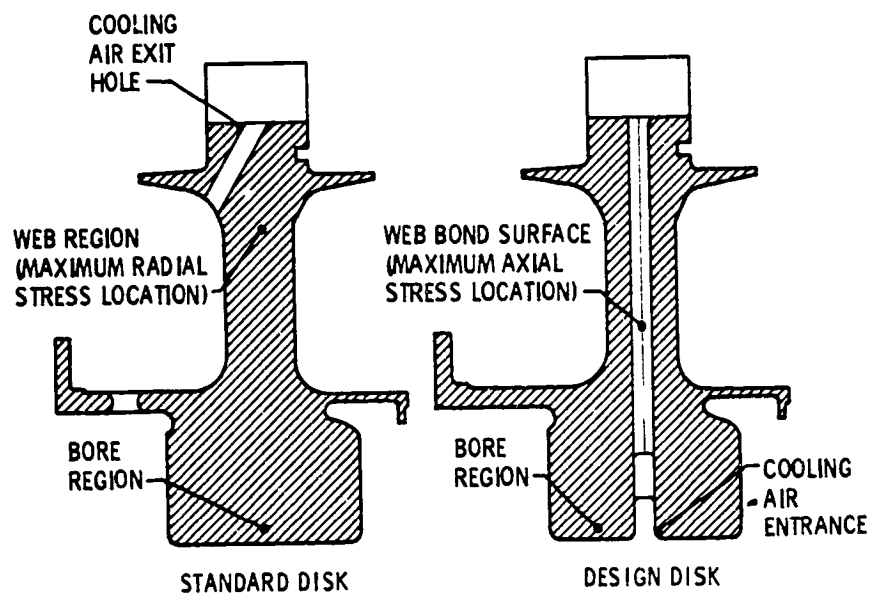


Figure 8. - JT8D-17 turbine disk assumed initial flaw locations.